International Journal for Parasitology: Drugs and Drug Resistance 24 (2024) 100531

Contents lists available at ScienceDirect

International Journal for Parasitology: Drugs and Drug Resistance

journal homepage: www.elsevier.com/locate/ijpddr

# Acrylonitrile derivatives: *In vitro* activity and mechanism of cell death induction against *Trypanosoma cruzi* and *Leishmania amazonensis*

Carlos J. Bethencourt-Estrella [a,b,c,*], Samuel Delgado-Hernández [d], Atteneri López-Arencibia [a,b,c], Desirée San Nicolás-Hernández [a,b], Lizbeth Salazar-Villatoro [e], Maritza Omaña-Molina [f], David Tejedor [d,**], Fernando García-Tellado [d], Jacob Lorenzo-Morales [a,b,c,***], José E. Piñero [a,b,c,****]

[a] *Instituto Universitario de Enfermedades Tropicales y Salud Pública de Canarias, Universidad de La Laguna, Avda. Astrofísico Fco. Sánchez, S/N, 38203 La Laguna, Islas Canarias, Tenerife, Spain*

[b] *Departamento de Obstetricia y Ginecología, Pediatría, Medicina Preventiva y Salud Pública, Toxicología, Medicina Legal y Forense y Parasitología, Universidad de La Laguna, Islas Canarias, Tenerife, Spain*

[c] *CIBER de Enfermedades Infecciosas (CIBERINFEC), Instituto de Salud Carlos III, 28029 Madrid, Spain*

[d] *Instituto de Productos Naturales y Agrobiología, Consejo Superior de Investigaciones Científicas, Avda. Fco. Sánchez 3, 38206 La Laguna, Islas Canarias, Tenerife, Spain*

[e] *Departamento de Infectómica y Patogénesis Molecular, Centro de Investigación y de Estudios Avanzados del Instituto Politécnico Nacional, Ciudad de Mexico 07360, Mexico*

[f] *Facultad de Estudios Superiores Iztacala, Medicina, Universidad Nacional Autónoma de México (UNAM), Tlalnepantla 54090, Mexico*

ARTICLE INFO

*Keywords:*
Chemotherapy
Toxicity
PCD
Leishmaniasis
Chagas
Acrylonitriles

ABSTRACT

Leishmaniasis and Chagas disease are parasitic infections that affect millions of people worldwide, producing thousands of deaths per year. The current treatments against these pathologies are not totally effective and produce some side effects in the patients. Acrylonitrile derivatives are a group of compounds that have shown activity against these two diseases. In this work, four novels synthetic acrylonitriles were evaluated against the intracellular form and extracellular forms of *L. amazonensis* and *T. cruzi*. The compounds 2 and 3 demonstrate to have good selectivity indexes against both parasites, specifically the compound 3 against the amastigote form (SI = 6 against *L. amazonensis* and SI = 7.4 against *T. cruzi*). In addition, the parasites treated with these two compounds demonstrate to produce a programmed cell death, since they were positive for the events studied related to this type of death, including chromatin condensation, accumulation of reactive oxygen species and alteration of the mitochondrial membrane potential. In conclusion, this work confirms that acrylonitriles is a source of possible new compounds against kinetoplastids, however, more studies are needed to corroborate this activity.

## 1. Introduction

The Chagas disease and Leishmaniasis are pathologies caused by trypanosomatids that produce severe problems in humans. Considered by the World Health Organisation (WHO) as Tropical Neglected Diseases (NTDs), leishmaniasis affects nearly 12 million people worldwide producing between 20 and 30 thousand deaths per year (de Vries and Schallig, 2022), while Chagas disease affects nearly 7 million people,

* Corresponding author. Instituto Universitario de Enfermedades Tropicales y Salud Pública de Canarias, Universidad de La Laguna, Avda. Astrofísico Fco. Sánchez, S/N, 38203, La Laguna, Tenerife, Islas Canarias, Spain.

** Corresponding author.

*** Corresponding author. Instituto Universitario de Enfermedades Tropicales y Salud Pública de Canarias, Universidad de La Laguna, Avda. Astrofísico Fco. Sánchez, S/N, 38203, La Laguna, Tenerife, Islas Canarias, Spain.

**** Corresponding author. Instituto Universitario de Enfermedades Tropicales y Salud Pública de Canarias, Universidad de La Laguna, Avda. Astrofísico Fco. Sánchez, S/N, 38203, La Laguna, Tenerife, Islas Canarias, Spain.

*E-mail addresses:* cbethene@ull.edu.es (C.J. Bethencourt-Estrella), dtejedor@ipna.csic.es (D. Tejedor), jmlorenz@ull.edu.es (J. Lorenzo-Morales), jpinero@ull.edu.es (J.E. Piñero).

https://doi.org/10.1016/j.ijpddr.2024.100531
Received 25 January 2024; Received in revised form 16 February 2024; Accepted 27 February 2024
Available online 6 March 2024

mainly in Latin America, producing 7 thousand deaths per year (Organizacion Mundial de la Salud (OMS), 2021).

Chagas disease is caused by the protozoan parasite *Trypanosoma cruzi,* discovered by Carlos Chagas in 1909. This disease is transmitted by the triatomine and causes a severe pathology that affects, in the chronic phase, the intestines and the heart (Bern, 2015). Leishmaniasis is caused by more than 20 species of *Leishmania*, which can produce different clinical manifestations, cutaneous, mucocutaneous and visceral forms, making patients' lives complicated from a health point of view, but also socio-economically, as they are limiting and produce psychosocial problems (Bennis et al., 2017).

Reference treatments for *Leishmania* include pentavalent antimonials, amphotericin B, miltefosine and paramomycin (Fernandes et al., 2022). For Chagas disease, the treatment is the same as that discovered 50 years ago, benznidazole and nifurtimox (Pérez-Molina et al., 2021). The treatments for these two pathologies are long and costly, lead to enormous side effects and are not totally effective.

This lack of activity and the high occurrence of side effects for these two pathologies, together with other factors such as the emergence of resistance and the high cost, have made the search for new treatments an essential task. In recent years, much research has focused on the search for new therapies to control leishmaniasis. These include, for example, marbofloxacin, a third-generation fluoroquinolone, and DDD853651/GSK3186899, a pyrazolopyrimidine (Sheikh et al., 2024). Natural compounds such as chalcones, alkaloids, quinolines and pyridines have also been shown to be effective against these parasites (Pal et al., 2023), with ursolic acid, coumarin, gallic acid and apigenin, among others, being particularly active (Afonso et al., 2023). In addition, other strategies such as the combination of drugs with immunotherapy have shown encouraging results. Within this group we can highlight rldccys1, a recombinant cysteine protease from *Leishmania*, or the use of *L. braziliensis* antigens with saponin and monophosphoryl lipid-A (Yadagiri et al., 2023). Similarly, there has been an increase in the number of studies related to the search for new therapies against Chagas disease. The use of antimicrobial peptides, such as mastoparan or crotalicidin (Hagemann et al., 2024), tryptophan derivatives, such as melatonin (Manful et al., 2024), or pharmacological repositioning, cholesterol-lowering treatments or antihistaminics, have shown good results in the treatment of *Trypanosoma cruzi* (Porta et al., 2023).

Acrylonitrile derivatives have been studied in recent decades for their potential use in different pathologies. It is a big group found in a multitude of drugs or natural products with diverse biological activities. This type of compounds have been shown to be active against viruses, such as dengue (Han et al., 2017) or HIV (Duan et al., 2020), or different bacteria (Saczewski et al., 2008), including mycobacterium tuberculosis (Sanna et al., 2000). Furthermore, they have also demonstrated activity as anticancer (Penthala et al., 2013) or anti-inflammatory agents (Sivaramakarthikeyan et al., 2020). In addition, different activities against parasites, such *Plasmodium* (Sharma et al., 2018), *Leishmania* spp. (Barbosa et al., 2009; Junior et al., 2010; Nakayama et al., 2007) or *Trypanosoma cruzi* (Sandes et al., 2010, 2014).

Previous reports demonstrate that acrylonitriles induce apoptosis when used to treat different pathologies (Dang et al., 2018; Kim and Choi, 2020; Luo et al., 2022; Tretyakova et al., 2019), including leishmaniasis and Chagas disease (Bethencourt-Estrella et al., 2021, 2022). Apoptotic cell death is described as a type of programmed and controlled cell death, which, in the case of parasitosis, avoids the possible inflammatory response that would occur in the hosts. This type of death is associated with some characteristic events, including chromatin condensation, decrease of ATP, alterations in the mitochondrial membrane potential, or production of oxidative stress, among others (Bruchhaus et al., 2007; Menna-Barreto, 2019).

In this work, four new acrylonitrile compounds were evaluated against *Trypanosoma cruzi* and *Leishmania amazonensis*, and the cytotoxicity was also studied to determine their selectivity. Moreover, the mechanism of cell death that these products produce in the parasites was also studied.

**Table 1**
Previous results of the activity and cytotoxicity of Q7, compound from which those studied in this work are derived (Bethencourt-Estrella et al., 2021, 2022).

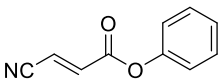


Q7

| | |
|---|---|
| $IC_{50}$: promastigote stage of *L. amazonensis* | 109.36 ± 4.74 μM |
| $IC_{50}$: epimastigote stage of *T. cruzi* | 15.52 ± 1.27 μM |
| $CC_{50}$: murine macrophages | 46.45 ± 3.81 μM |

$IC_{50}$: inhibitory concentration 50; $CC_{50}$: cytotoxic concentration 50.

## 2. Materials and methods

### 2.1. Chemical

All reagents from commercial suppliers were used without further purification. All solvents were freshly distilled before use from appropriate drying agents. Analytical TLCs were performed with silica gel 60 F254 plates. Visualization was accomplished by UV light. Column chromatography was carried out using silica gel 60 (230–400 mesh ASTM). NMR spectra were obtained on a Bruker Avance 400 MHz spectrometers and recorded at 25 °C. Chemical shifts for $^{1}$H NMR spectra are reported in ppm, chemical shifts for $^{13}$C NMR spectra are recorded in ppm relative to internal deuterated chloroform ($\delta = 77.2$ ppm for $^{13}$C). Coupling constants (J) are reported in Hertz. The terms m, s, d, t, q refers to multiplet, singlet, doublet, triplet, quartet. $^{13}$C NMR were broadband decoupled from hydrogen nuclei. High resolution mass spectra (HRMS) was measured by EI method with a Agilent LC-Q-TOF-MS 6520 spectrometer.

The 4 tested novel compounds are acrylonitriles derivatives of **Q7**, previously reported for its activity against trypanosomatids (Table 1), producing apoptotic-like cell death. These compounds were synthetized as described by the original process (Tejedor et al., 2019). All the compounds were dissolved in dimethyl sulfoxide (DMSO) (Merck, Darmstad, Germany) and stored in the dark at −20 °C.

### 2.2. Cultures

The parasites used in this work include promastigote forms of *Leishamania amazonensis* (MHOM/BR/77/LTB0016) cultured at 26 °C in Schneider's medium (SND) (Sigma-Aldrich, Darmstadt, Germany) supplemented with a 10% of foetal bovine serum (FBS) and epimastigote forms of *Trypanosoma cruzi* (Y strain) cultured at 26 °C in Liver Infusion Tryptose (LIT) supplemented with a 10% of FBS. For the cytotoxicity assays murine macrophages (J774A.1) were used, cultured at 37 °C with a 5% $CO_2$ atmosphere in Dulbecco's Modified Eagle Medium (DMEM) supplemented with a 10% of FBS.

### 2.3. Antiparasitic activity

The antiparasitic activity was developed against *Trypanosoma cruzi* and *Leishmania amazonensis.* To develop the activity against the extracellular forms of the parasites, epimastigote forms of *Trypanosoma cruzi* and promastigote forms of *Leishmania amazonensis* were used. In sterile 96 well plates, serial dilutions of the compounds were added with quantity of $10^5$ parasites per well in the growth medium of each parasite (LIT for *T. cruzi* and SND for *L. amazonensis*) reaching a finale volume of 200 μl per well. A 10 % of alamarBlue Cell Viability Reagent® (ThermoFisher Scientific, Waltham, MA, USA) was added. After 72 h at 26 °C, the fluorescence of each well (544 nm excitation, 590 nm emission) was determine using the EnSpire Multimode Plate Reader® (PerkinElmer, Thermo Fischer Scientific, Madrid, Spain). The inhibitory concentration 50 ($IC_{50}$), concentration which inhibits the 50% of the parasite

population, was calculated using a nonlinear regression analysis in the Graphpad Prism 9.0.0. (López-Arencibia et al., 2019a).

To develop the activity against the intracellular forms of the parasites, the amastigote forms, the same colorimetric method, based on the alamarBlue reagent was used. In 96 well plates, $10^4$ murine macrophages per well with a high concentration of the parasites were added ($10^5$ for promastigote forms of *L. amazonensis* and $5 \times 10^4$ for epimastigote forms of *T. cruzi*) in DMEM medium. After incubating at 37 °C in 5% of $CO_2$ atmosphere (24 h for *L. amazonensis* and 48 h in the case of *T. cruzi*) to promote the infection of the macrophages, the plates were washed to eliminate the non-internalized parasites, and serial dilutions of the compounds to test were added (previously prepared in DMEM in a deepwell). After 24 h of treatment, the compounds were removed and 30 µl of 0,05% SDS in medium (LIT for *T. cruzi* and SND for *L.* amazonensis) were added to produce the lysis of the macrophages. After 30 s, medium was added to reach 200 µl and disrupt the activity of the SDS. Finally, a 10% of alamarBlue reagent was added and the plates were incubated at 26 °C for 72 h. The fluorescence was measured using the EnSpire Multimode Plate Reader® to calculate the $IC_{50}$ of the compounds (Bethencourt-Estrella et al., 2023).

### 2.4. Cytotoxicity against murine macrophages

To determine de cytotoxic concentration 50 ($CC_{50}$), concentration that inhibits the growth of the 50% of the cell population, a colorimetric method based on the alamarBlue reagent was used. In a 96 well plates, $10^4$ macrophages per well were added. After 3–4 h to complete the adherence of the cells, serial dilutions of the compounds were added in a finale volume of 100 µl with a 10% of alamarBlue reagent. After an incubation of 24 h at 37 °C and 5% of $CO_2$ atmosphere, the fluorescence was measured using the EnSpire Multimode Plate Reader® and the $CC_{50}$ was calculated using the Graphpad Prism 9.0.0. (López-Arencibia et al., 2019b).

At this point, with the results of $CC_{50}$ and $IC_{50}$ the selectivity index can be calculated, which reports how much selective were the compounds for parasites rather than mammal's cells.

### 2.5. Mechanisms of cell death

The most selective compounds, the acrylonitrile 2 and 3, were chosen to study the type of cell death produced in the parasites. To perform these assays different kits were used to demonstrate different events involved in a programmed cell death. To carry out these assays, the parasites ($10^6$ cells/ml) were incubated with the $IC_{90}$ of the most selective compounds at 26 °C for 24 h. After this incubation, the kits were following the manufacturer's instructions.

### 2.6. Chromatin condensation analysis

To determine the presence of chromatin condensation the Vybrant® Apoptosis Assay Kit n∘5 (ThermoFisher Scientific, MA, USA) was used. This kit has two stains, the Hoechst 33,342, which dye on blue the chromatin condensed, and the Propidium Iodide (PI), the one that dye on red the death cells. After the incubation with the $IC_{90}$ of the compounds, centrifugation was carried out (3000 rpm, 10 min, 4 °C), and the treated cells were resuspended in 50 µl of buffer. The Hoechst (5 µg/ml) and the PI (1 µg/ml) were added and, after 20 min of incubation at 26 °C, some pictures were captured with the EVOS® FL Cell Imaging System (ThermoFisher Scientific, MA, USA) using DAPI (excitation 350 nm/emission 461 nm, for Hoechst) and RFP (excitation 535 nm/emission 617 nm, for PI) light cubes (Bethencourt-Estrella et al., 2023).

### 2.7. Mitochondrial membrane potential analysis

The JC-1 Mitochondrial Membrane Potential Assay Kit® (Cayman Chemical, Ann Arbor, MI, USA) was used to detect changes in the mitochondrial membrane potential of the cells. After the incubation, the treated cells were centrifuged (3000 rpm, 10 min, 4 °C) and resuspended in 50 µl of buffer in a black plate. 5 µl of JC-1 was added and, after 30 min of incubation, the green (J-monomers, excitation 540 nm/emission 470 nm) and red (J-aggregates, excitation 485 nm/emission 535 nm) fluorescence were measured, and the result were expressed as percentage relative to the negative control of the ratio red/green fluorescence. A positive control was added, carbonyl cyanide m-chlorophenyl hydrazone (CCCP, 100 µM for 3 h) and a reference treatment, miltefosine for *L. amazonensis* and benznidazole for *T. cruzi* (García-Davis et al., 2023).

### 2.8. Analysis of ATP levels

CellTiter-Glo® Luminescent Cell Viability Assay (Promega, WI, USA) was used to detect variations in the levels of ATP. After the incubation, the treated parasites were centrifuged (3000 rpm, 10 min, 4 °C) and resuspended in 25 µl of buffer in a white plate with another 25 µl of the kit. After 10 min of incubation at room temperature, the luminescent was determined using EnSpire Multimode Plate Reader® (PerkinElmer). The results were expressed in percentage to the negative control, without treatment. Sodium azide ($NaN_3$ 20 mM for 3 h) was added as a positive control and miltefosine (*L. amazonensis*) and benznidazole (*T. cruzi*) as a reference treatments (López-Arencibia et al., 2021).

### 2.9. Integrity of the membrane permeability analysis

SYTOX® Green nucleic acid stain fluorescent dye (ThermoFisher Scientific, MA, USA) was used to elucidate if the plasmatic membrane permeability is altered. To develop the assay, the treated cells were centrifuged (3000 rpm, 10 min, 4 °C), resuspended in 50 µl of buffer and the kit was added at a final concentration of 1 µM. After 15 min of incubation at room temperature, fluorescence pictures were taken with EVOS® FL Cell Imaging System (ThermoFisher Scientific, MA, USA) in the GFP light cube (excitation 504 nm/emission 523 nm). Triton 0.1 % was used as a positive control and a reference treatment was added (Benznidazol for *T. cruzi* and Miltefosine for *L. amazonensis*) (San Nicolás-Hernández et al., 2023b).

### 2.10. Analysis of the presence of reactive oxygen species

CellROX® Deep Red Reagent (ThermoFisher Scientific, MA, USA) was used to analyze the oxidative stress. After the 24 h of incubation with the compounds, the parasites were centrifuged (3000 rpm, 10 min, 4 °C), resuspended in 50 µl of buffer and incubated at 5 µM of CellROX reagent for 30 min. Then, the presence of reactive oxygen species was detected with the EVOS® FL Cell Imaging System (ThermoFisher Scientific, MA, USA) in the Cy5 light cube (excitation 644 nm/emission 665 nm). Hydrogen peroxide ($H_2O_2$ 600 mM for 30 min) was used as a positive control and the reference treatments were also added (Benznidazol for *T. cruzi* and Miltefosine for *L. amazonensis*) (San Nicolás-Hernández et al., 2023a).

### 2.11. Transmission electron microscopy (TEM)

Transmission electron microscopy was used to develop the analysis of the ultrastructural changes of the treated cells. To see the morphological damage caused in the parasites JEOL JEM-1011 transmission electron microscope (JEOL Ltd., Tokyo, Japan) was used (Castelan-Ramírez et al., 2020). The assay was developed incubating the parasites with the $IC_{90}$ of the compounds for 24 h. The samples were fixed with 2.5% glutaraldehyde and then fixed with 1% osmium tetroxide in cacodylate. The dehydration was done with ethanol and the parasites were embedded in epoxy resins. Finally, the thin sections were observed in transmission electron microscope (González-Robles et al., 2012). The TEM was developed in collaboration with the Facultad de Estudios Superiores Iztacala (FESI), Medicina, UNAM, Mexico

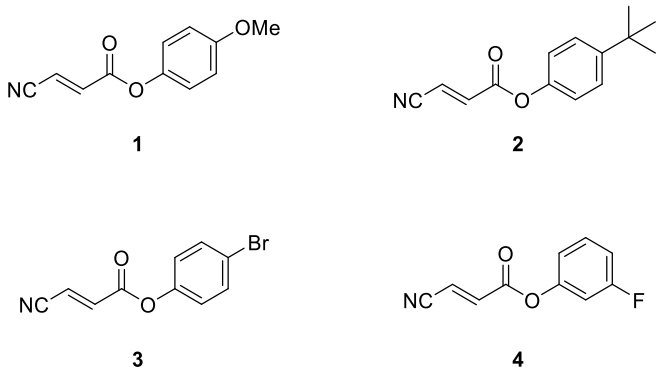


**Fig. 1.** Acrylonitriles synthetized and studied in this work.

(Nicolás-Hernández et al., 2023).

### 2.12. Statistical analysis

The inhibitory concentrations ($IC_{50}$ and $IC_{90}$) and cytotoxic concentration ($CC_{50}$) were determined using a non-linear regression [Inhibitor] vs response – Variable slope (four parameters) by non-linear regression analysis with 95 % confidence, using the GraphPad Prism 9.0.0 statistical software. The experiments were performed in duplicate in three different days. The analysis was developed using a Tukey's test, considering significant values of $p < 0.05$. The ANOVA analysis was also done in the GraphPad Prism 9.0.0.

## 3. Results

### 3.1. Chemical

The tested novel compounds, **1–4** (Fig. 1), are acrylonitriles derivatives of **Q7**, synthetized following the general procedure (Coles et al., 2018); to a solution of alkyne (2.0 mmol), acetone cyanohydrin (2.1 mmol) and DABCO (0.020 mmol) in $CH_2Cl_2$ (4 ml) was stirred for 1 h at room temperature (Scheme 1). Solvent was evaporated under reduced pressure and the crude residue was flash chromatographed using silica gel. Elution with ethylacetate/hexanes (10:90 v/v) afforded the desired pure product (characterization in the supporting information). Their purity was confirmed by NMR spectroscopy (characterization in the supporting information).

### 3.2. Antiparasitic activity

The activity of the four acrylonitriles was studied against extracellular forms of *Leishmania amazonensis* and *Trypanosoma cruzi*. The results of the inhibitory concentration 50 ($IC_{50}$), the concentration which inhibits the 50% of the population of parasites, against the promastigote form of *L. amazonensis* and the epimastigote form of *T. cruzi* were included in Table 2.

As well, the activity against the intracellular forms of the parasites

**Table 2**
Activity against extracellular forms, promastigote stage of *L. amazonensis* and epimastigote stage of *Trypanosoma cruzi*.

| | Structure | $IC_{50}$ (μM) Promastigote (*L. amazonensis*) | $IC_{50}$ (μM) Epimastigote (*T. cruzi*) |
|---|---|---|---|
| 1 | 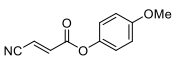 | 27.08 ± 1.88 | 10.16 ± 0.97 |
| 2 | 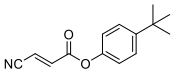 | 20.03 ± 4.74 | 12.32 ± 2.11 |
| 3 | 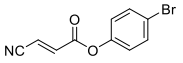 | 8.14 ± 1.2 | 17.52 ± 1.71 |
| 4 | 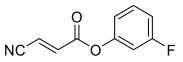 | 28.39 ± 5.2 | 5.06 ± 1.11 |
| M | 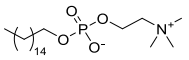 | 6.48 ± 0.25 | |
| B | 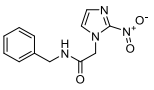 | | 6.92 ± 0.77 |

$IC_{50}$: inhibitory concentration 50; M: miltefosine, reference drug for *L. amazonensis*; B: benznidazole, reference drug for *T. cruzi*.

**Table 3**
Activity against intracellular forms, amastigote stage of *L. amazonensis* and *Trypanosoma cruzi*.

| | $IC_{50}$ (μM) Amastigote (*L. amazonensis*) | $IC_{50}$ (μM) Amastigote (*T. cruzi*) |
|---|---|---|
| 1 | 45.83 ± 3.61 | 92.30 ± 12.14 |
| 2 | 67.25 ± 1.73 | 23.08 ± 4.77 |
| 3 | 18.13 ± 3.53 | 14.86 ± 4.33 |
| 4 | 48.00 ± 2.8 | 127.9 ± 8.03 |
| M | 3.12 ± 0.30 | |
| B | | 2.67 ± 0.39 |

$IC_{50}$: inhibitory concentration 50; M: miltefosine, reference drug for *L. amazonensis*; B: benznidazole, reference drug for *T. cruzi*.

**Table 4**
Cytotoxicity of the studied compounds.

| | $CC_{50}$ (μM) |
|---|---|
| 1 | 38.75 ± 7.28 |
| 2 | 79.53 ± 12.14 |
| 3 | 109.39 ± 24.57 |
| 4 | 34.02 ± 7.71 |
| B | 399.91 ± 1.40 |
| M | 72.18 ± 8.85 |

$CC_{50}$: inhibitory concentration 50; M: miltefosine, reference drug for *L. amazonensis*; B: benznidazole, reference drug for *T. cruzi*.

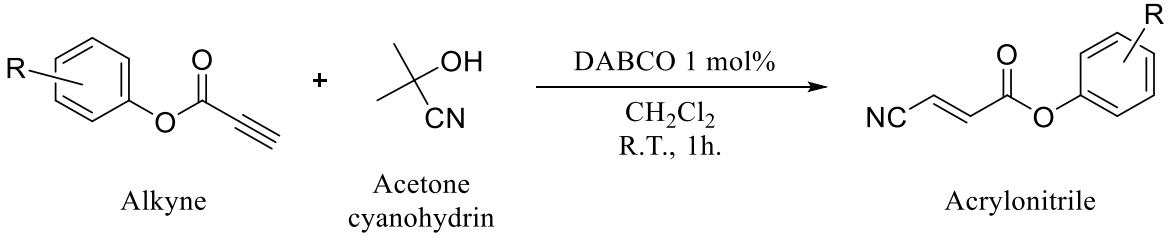


**Scheme 1.** General procedure to obtain the acrylonitriles studied (Coles et al., 2018; Tejedor et al., 2019).

**Table 5**
Activity against extracellular and intracellular forms of *L. amazonensis* and *Trypanosoma cruzi*.

| | SI (*L. amazonensis*) | | SI (*T. cruzi*) | |
|---|---|---|---|---|
| | Promastigote | Amastigote | Epimastigote | Amastigote |
| 1 | 1.4 | 0.9 | 3.8 | 0.4 |
| 2 | 4.0 | 1.2 | 6.5 | 3.5 |
| 3 | 13.4 | 6.0 | 6.2 | 7.4 |
| 4 | 1.2 | 0.7 | 6.7 | 0.3 |
| M | 11.1 | 23.1 | | |
| B | | | 57.8 | 149.8 |

SI: selectivity index $CC_{50}/IC_{50}$; M: miltefosine, reference drug for *L. amazonensis*; B: benznidazole, reference drug for *T. cruzi*.

was developed. The $IC_{50}$ against the amastigote stage of *L. amazonensis* and *T. cruzi* were presented in Table 3.

### 3.3. Cytotoxicity against murine macrophages

The toxicity produced by these acrylonitriles was developed against murine macrophages. The results of cytotoxic concentration 50 ($CC_{50}$), concentration that inhibits the growth of the 50% of the cell population, were included in Table 4.

In addition, considering the values of $IC_{50}$ and $CC_{50}$, the selectivity of the tested compounds against intracellular and extracellular forms of the parasites was studied. The selectivity index (SI), the ratio $CC_{50}/IC_{50}$, were included in Table 5.

### 3.4. Mechanisms of cell death

Compounds 2 and 3 demonstrate the best activity-cytotoxicity relationship, with the highest selectivity index values, and for this reason, these two compounds were chosen to determine the type of death they produce in the parasites.

### 3.5. Chromatin condensation analysis

To determine the presence of chromatin condensation the double stain Vybrant™ Apoptosis Assay Kit was used. The propidium iodide, which shows on red the death cells, can be displayed in the RFP channel, the Hoechst, which shows chromatin condensed on blue, can be visualized in the DAPI channel, and, in addition, the morphology of the parasites can be observed in the transmitted light channel. The results of the incubation of this kit with compounds 2 and 3 against *L. amazonensis* and *T. cruzi*, were presented in Figs. 2 and 3, respectively.

### 3.6. Mitochondrial membrane potential analysis

To determine the alteration in the mitochondrial membrane potential the JC-1 Mitochondrial Membrane Potential Assay Kit® was used. The results were expressed in percentage of mitochondrial membrane potential relative to the negative control (without treatment) in the following graphs (Figs. 4 and 5).

### 3.7. Analysis of ATP levels

To analyze the variations in the levels of ATP the CellTiter-Glo® Luminescent Cell Viability Assay kit was used. The results of percentage of ATP relative to the negative control were included in these graphs (Figs. 6 and 7).

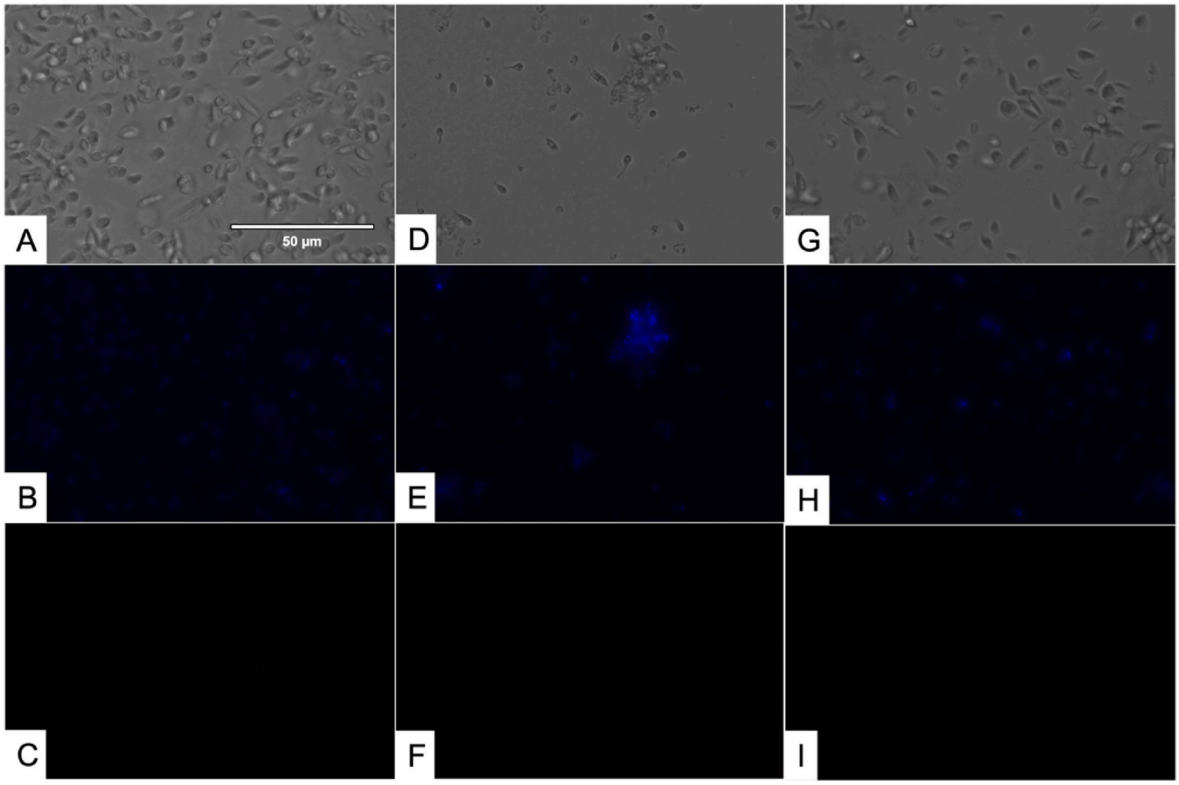


**Fig. 2.** Results of Hoechst–propidium iodide staining in treated parasites. Results after 24 h of incubation of promastigotes of *L. amazonensis* against the $IC_{90}$ of acrylonitriles. Images were captured using an EVOS FL Cell Imaging System (40×). Scale-bar: 50 µm. A: Non treated parasites in visible channel; B: Non treated parasites in DAPI channel; C: Non treated parasites in RFP channel; D: Parasites treated with acrylonitrile 2 in visible channel; E: Parasites treated with acrylonitrile 2 in DAPI channel; F: Parasites treated with acrylonitrile 2 in RFP channel; G: Parasites treated with acrylonitrile 3 in visible channel; H: Parasites treated with acrylonitrile 3 in DAPI channel; I: Parasites treated with acrylonitrile 3 in RFP channel.

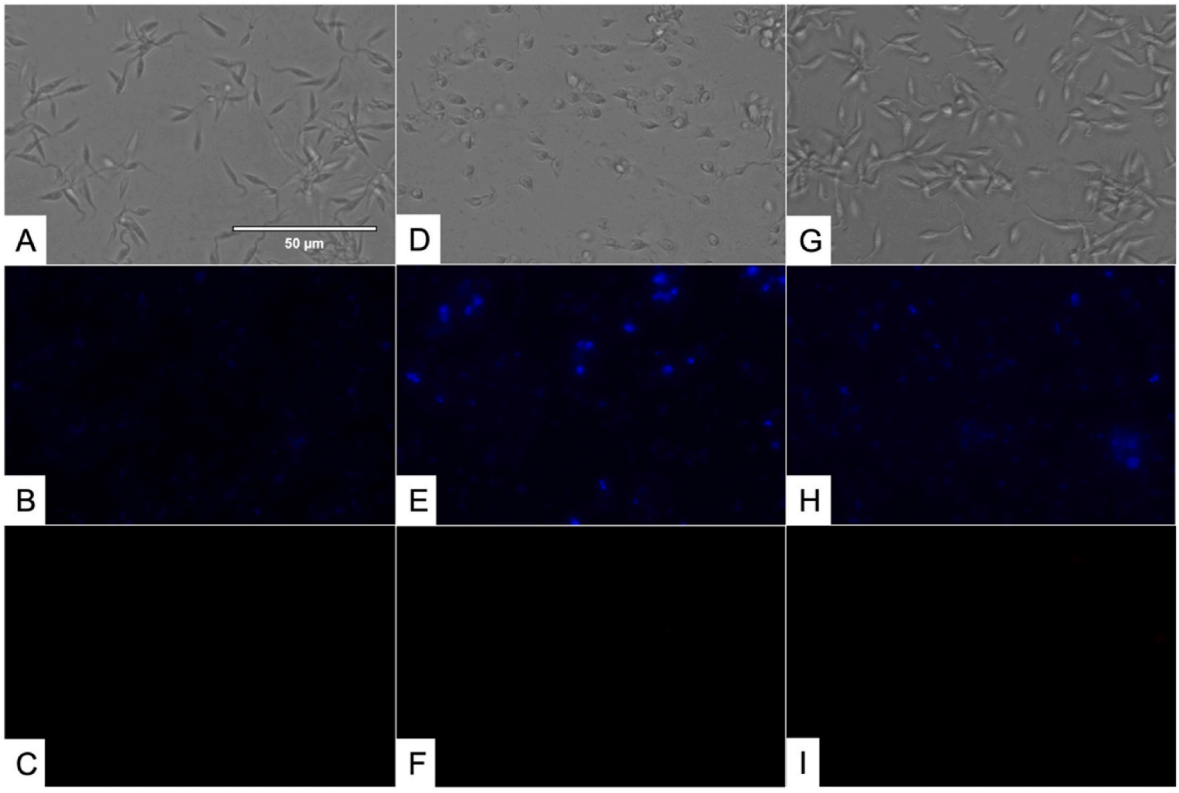


**Fig. 3.** Results of Hoechst–propidium iodide staining in treated parasites. Results after 24 h of incubation of epimastigotes of *T. cruzi* against the $IC_{90}$ of acrylonitriles. Images were captured using an EVOS FL Cell Imaging System (40×). Scale-bar: 50 µm. A: Non treated parasites in visible channel; B: Non treated parasites in DAPI channel; C: Non treated parasites in RFP channel; D: Parasites treated with acrylonitrile 2 in visible channel; E: Parasites treated with acrylonitrile 2 in DAPI channel; F: Parasites treated with acrylonitrile 2 in RFP channel; G: Parasites treated with acrylonitrile 3 in visible channel; H: Parasites treated with acrylonitrile 3 in DAPI channel; I: Parasites treated with acrylonitrile 3 in RFP channel.

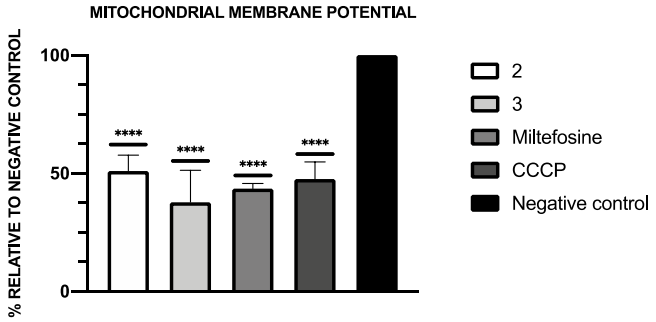


**Fig. 4.** Results of mitochondrial membrane potential alterations (△Ψm) expressed as percentage relative to negative control (C-), carbonyl cyanide m-chlorophenyl hydrazone (CCCP), positive control, and miltefosine, the reference treatment, were added. A Tukey test with the GraphPad.PRISM® 9.0.0 software was done to test the statistical differences between means. ($p < 0.0001$ [****]). All experiments were performed in duplicate in three different days. 2: Parasites treated for 24 h with the $IC_{90}$ of the acrylonitrile 2; 3: Parasites treated for 24 h with the $IC_{90}$ of the acrylonitrile 3.

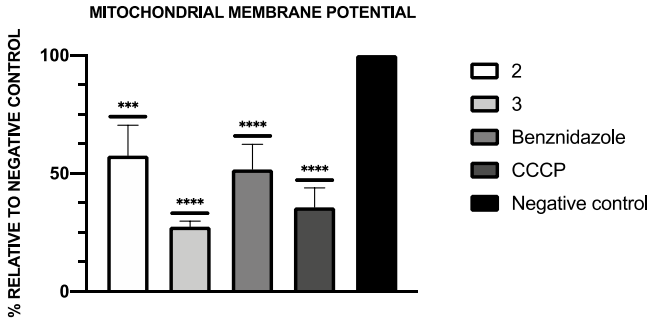


**Fig. 5.** Results of mitochondrial membrane potential alterations (△Ψm) expressed as percentage relative to negative control (C-), carbonyl cyanide m-chlorophenyl hydrazone (CCCP), positive control, and benznidazole, the reference treatment, were added. A Tukey test with the GraphPad.PRISM® 9.0.0 software was done to test the statistical differences between means. ($p < 0.0001$ [****]). All experiments were performed in duplicate in three different days. 2: Parasites treated for 24 h with the $IC_{90}$ of the acrylonitrile 2; 3: Parasites treated for 24 h with the $IC_{90}$ of the acrylonitrile 3.

### *3.8. Integrity of the membrane permeability analysis*

To determine whether the integrity of the membrane is maintained after treatment, the Sytox® Green kit was used. Alterations in the integrity of the membrane allow the stain to enter in the cells emitting green fluorescence, which can be observed in the GFP channel (Figs. 8 and 9).

### *3.9. Analysis of the presence of reactive oxygen species*

To demonstrate the presence of reactive oxygen species the CellROX® Deep Red Reagent was used. The presence of red fluorescence, which indicates presence of reactive oxygen species, can be observed in Fig. 10, against *L. amazonensis,* and Fig. 11, against *T. cruzi*.

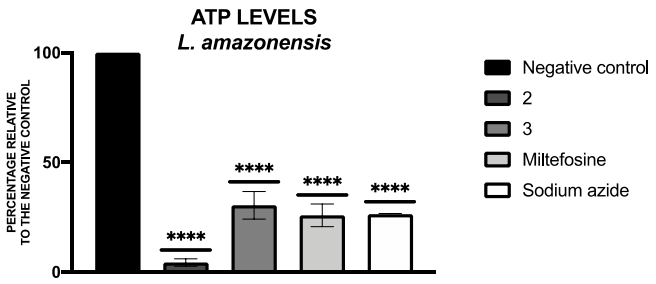


**Fig. 6.** Results of the ATP levels represented as the percentage relative to negative control, miltefosine was used as the reference treatment, and sodium azide was used as positive control. A Tukey test with the GraphPad.PRISM® 9.0.0 software was done to test the statistical differences between means. ($p < 0.0001$ [****]). 2: Parasites treated for 24 h with the $IC_{90}$ of the acrylonitrile 2; 3: Parasites treated for 24 h with the $IC_{90}$ of the acrylonitrile 3.

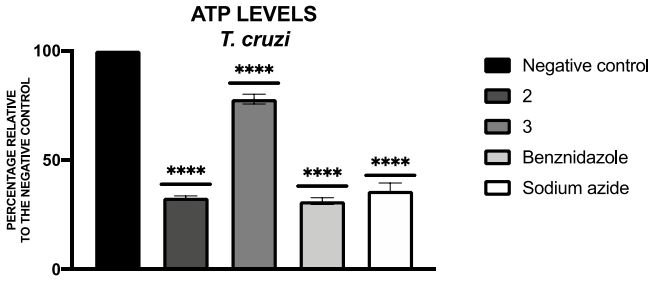


**Fig. 7.** Results of the ATP levels represented as the percentage relative to negative control, benznidazole was used as the reference treatment, and sodium azide was used as positive control. A Tukey test with the GraphPad.PRISM® 9.0.0 software was done to test the statistical differences between means. ($p < 0.0001$ [****]). 2: Parasites treated for 24 h with the $IC_{90}$ of the acrylonitrile 2; 3: Parasites treated for 24 h with the $IC_{90}$ of the acrylonitrile 3.

### 3.10. Transmission electron microscopy (TEM)

To evaluate the morphological alterations and the ultrastructural produced in promastigotes of *L. amazonensis* and epimastigotes of *T.* cruzi by the tested compounds, the transmission electron microscopy (TEM) was used (Figs. 12 and 13).

In the images of *L. amazonensis* (Fig. 12), it is possible to observe in untreated parasites (Fig. 12A) the characteristic morphological elongated form of the promastigotes, normal nucleus without condensation and well conditions of the rest of the organelles. In the parasites treated with the $IC_{90}$ of the compounds 2 (Fig. 12B and C) and 3 (Fig. 12D–F) some morphological changes are shown. The most visible feature is the change in the general morphology of the cells, the treated cells lost the characteristic elongated form, appearing to be rounding and swelling, but preserving the plasmatic membrane. Additionally, the cell interior is in disarray, without cytoplasmic content, with clear signs of organelle digestion which makes it difficult to differentiate between organelles.

More in depth, talking about specific organelles with genetic material, disorganization of the nucleus can be observed (Fig. 12B and C), as well as the loss of shape of the kinetoplast (K), which is observed to be enlarged (Fig. 12C and F). In addition, two nuclei can be observed in the same cell (Fig. 12F), which would indicate an alteration in the normal development of the life cycle.

Other important changes are seen in the flagellum (F) and flagellar pocket (FP) (Fig. 12B), which could affect the motility of the parasite. As well as an increase in the amount of reservosomes (R), lipid bodies that may be associated with the protection of the cell by building up energy reserves.

In the case of the negative control of *T. cruzi* (Fig. 13A), the morphological characteristic elongated form of the epimastigotes is also maintained, and the organelles can be observed in perfect conditions as well. Seeing the images of parasites treated with the $IC_{90}$ of the compounds 2 (Fig. 13B–E) and 3 (Fig. 13F–I), some damages and changes compared to the negative control can be observed.

The most ultrastructural change observed is the loss of the elongated form, the treated epimastigotes take a rounded shape (Fig. 13B and F), also the alteration of the continuity of the cytoplasm is noticeable in treated parasites.

As well as in the case of *L. amazonensis,* organelles present some alterations. The enlargement of the kinetoplast (K), the disruption in the flagellum (F) and flagellar pocket (FP), the increase in the number of reservosomes (R) or the loss of shape of the nucleus are presented. Moreover, the condensation of the treated nuclei also appears (*).

In addition, the non-characteristic elongated and distended form of endoplasmic reticulum (ER) (Fig. 13C and F), the presence of multilamellar bodies (MB) and the huge number of vacuoles (V) can be observed in treated epimastigotes.

## 4. Discussion

Acrylonitriles have been shown to be a source of compounds with numerous biological activities. They have shown anti-inflammatory

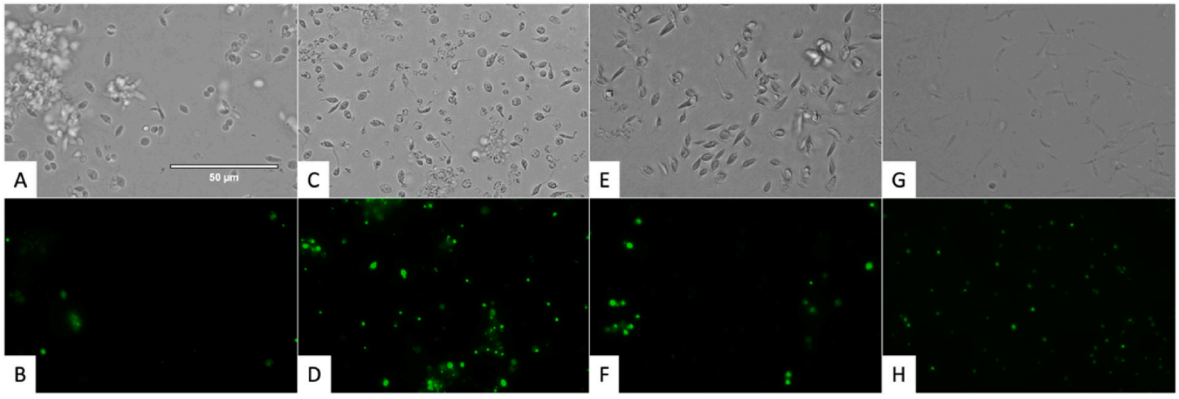


**Fig. 8.** Detection of plasmatic membrane permeability using SYTOX® Green staining in promastigote stage of *L. amazonensis*. Images were captured using an EVOS FL Cell Imaging System (40×). Scale-bar: 50 µm. A: Non treated parasites in visible channel; B: Non treated parasites in GFP channel; C: Parasites treated with acrylonitrile 2 in visible channel; D: Parasites treated with acrylonitrile 2 in GFP channel; E: Parasites treated with acrylonitrile 3 in visible channel; F: Parasites treated with acrylonitrile 3 in GFP channel; G: Parasites treated with Triton 0.1%, positive control, in visible channel. H: Parasites treated with Triton 0.1%, positive control, in GFP channel.

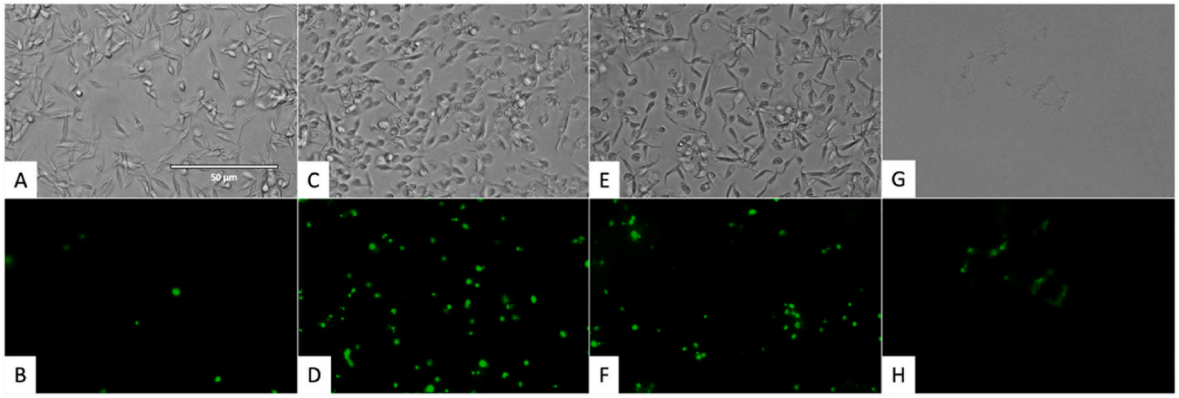


**Fig. 9.** Detection of plasmatic membrane permeability using SYTOX® Green staining in epimastigote stage of *T. cruzi*. Images were captured using an EVOS FL Cell Imaging System (40×). Scale-bar: 50 µm. A: Non treated parasites in visible channel; B: Non treated parasites in GFP channel; C: Parasites treated with acrylonitrile 2 in visible channel; D: Parasites treated with acrylonitrile 2 in GFP channel; E: Parasites treated with acrylonitrile 3 in visible channel; F: Parasites treated with acrylonitrile 3 in GFP channel; G: Parasites treated with Triton 0.1%, positive control, in visible channel. H: Parasites treated with Triton 0.1%, positive control, in GFP channel.

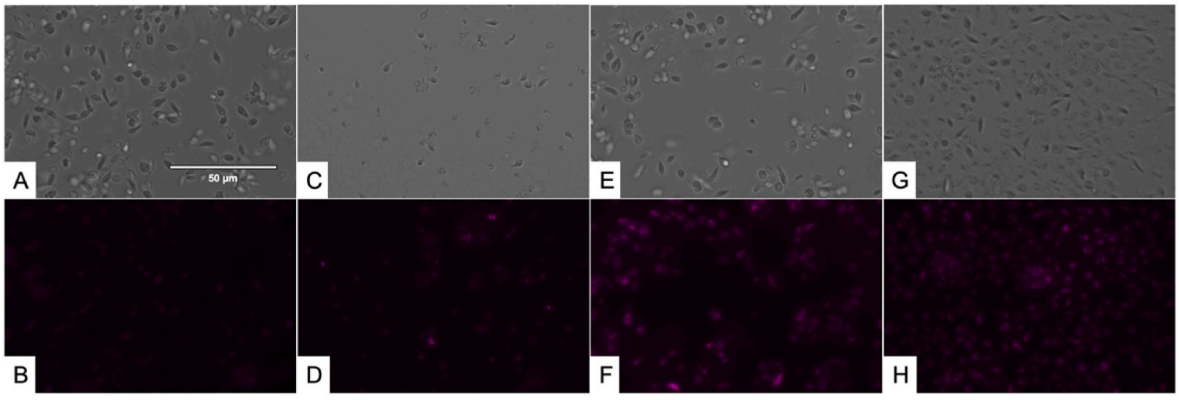


**Fig. 10.** Detection of reactive oxygen species using CellROX® Deep Red staining in promastigote stage of *L. amazonensis*. Images were captured using an EVOS FL Cell Imaging System (40×). Scale-bar: 50 µm. A: Non treated parasites in visible channel; B: Non treated parasites in Cy5 channel; C: Parasites treated with acrylonitrile 2 in visible channel; D: Parasites treated with acrylonitrile 2 in Cy5 channel; E: Parasites treated with acrylonitrile 3 in visible channel; F: Parasites treated with acrylonitrile 3 in Cy5 channel; G: Parasites treated with $H_2O_2$ 600 mM, positive control, in visible channel. H: Parasites treated with $H_2O_2$ 600 mM, positive control, in Cy5 channel.

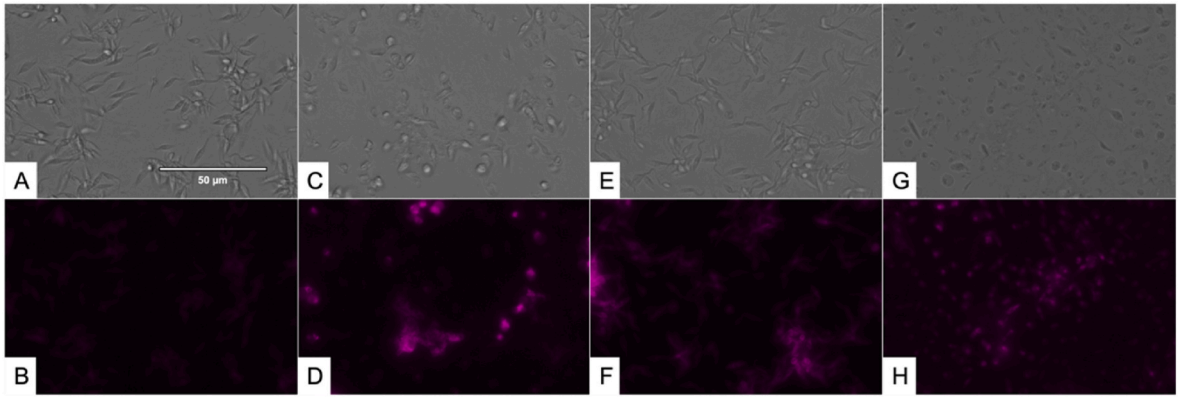


**Fig. 11.** Detection of reactive oxygen species using CellROX® Deep Red staining in epimastigote stage of *T. cruzi*. Images were captured using an EVOS FL Cell Imaging System (40×). Scale-bar: 50 µm. A: Non treated parasites in visible channel; B: Non treated parasites in Cy5 channel; C: Parasites treated with acrylonitrile 2 in visible channel; D: Parasites treated with acrylonitrile 2 in Cy5 channel; E: Parasites treated with acrylonitrile 3 in visible channel; F: Parasites treated with acrylonitrile 3 in Cy5 channel; G: Parasites treated with $H_2O_2$ 600 mM, positive control, in visible channel. H: Parasites treated with $H_2O_2$ 600 mM, positive control, in Cy5 channel.

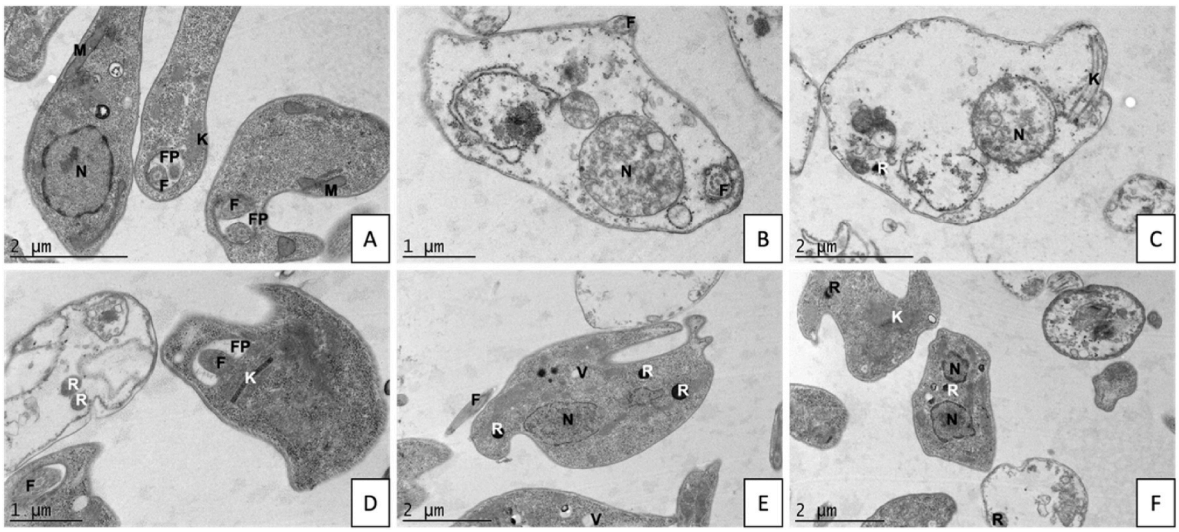


**Fig. 12.** Ultraestructural analysis of transmission electron microscopy of *L. amazonensis* treated with the $IC_{90}$ of acrylonitriles for 24 h. A: Non treated parasites; B and C: Parasites treated with acrylonitrile 2; D, E and F: Parasites treated with acrylonitrile 3. In the images, some organelles were observed (M: Mitochondria; N: Nuclei; FP: Flagellar pocket; F: Flagellum; K: Kinetoplast; R: Reservosome; V: Vacuole).

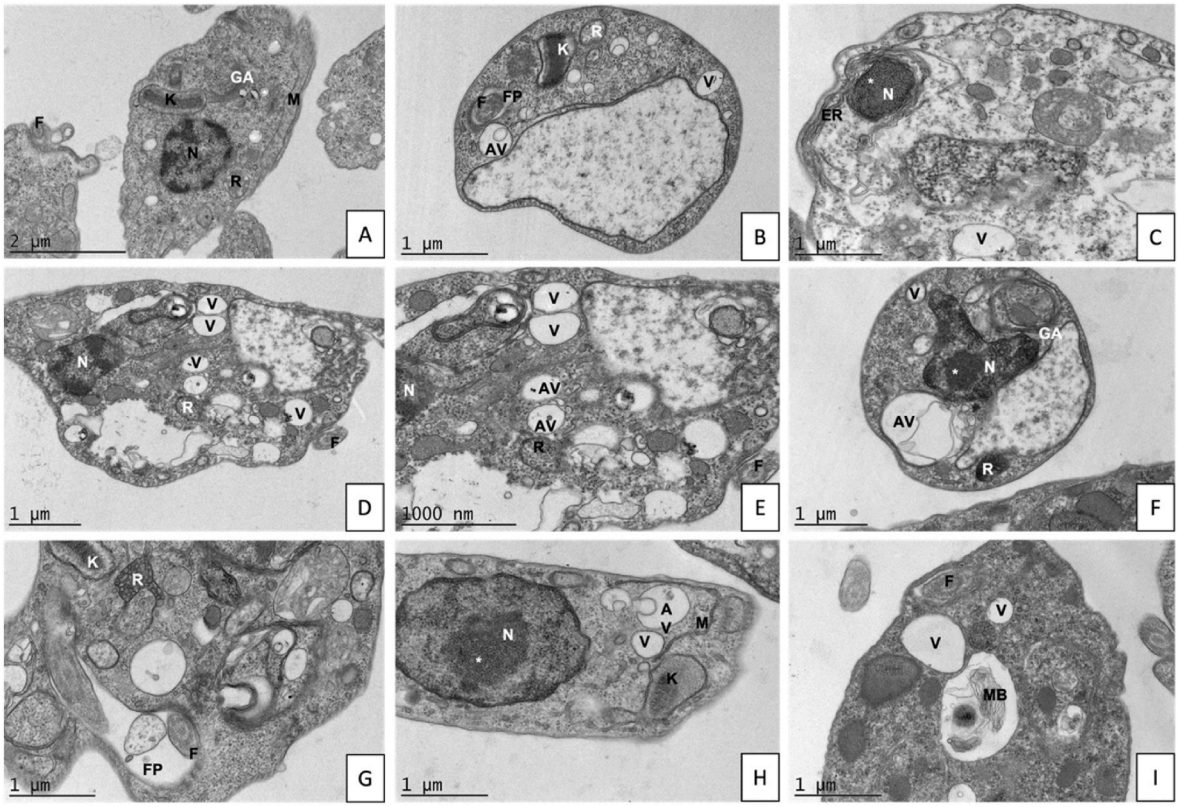


**Fig. 13.** Ultraestructural analysis of transmission electron microscopy of *T. cruzi* treated with the $IC_{90}$ of acrylonitriles for 24 h. Images were captured using JEOL JEM-1011 transmission electron microscope. A: Non treated parasites; B, C, D and E: Parasites treated with acrylonitrile 2; F, G, H and I: Parasites treated with acrylonitrile 3. In the images, some organelles were observed (M: Mitochondria; N: Nuclei; GA: Golgi apparatus; FP: Flagellar pocket; F: Flagellum; K: Kinetoplast; R: Reservosome; V: Vacuole; MB: Multilamellar bodies; AV: Autophagic vacuole; *: Chromatin condensation).

(Sivaramakarthikeyan et al., 2020) and anticancer (Penthala et al., 2013) activity, as well as numerous activities against microorganisms such as viruses (Duan et al., 2020; Han et al., 2017), bacteria (Saczewski et al., 2008; Sanna et al., 2000) or parasites (Barbosa et al., 2009; Junior et al., 2010; Nakayama et al., 2007; Sandes et al., 2010, 2014; Sharma et al., 2018).

The four compounds studied demonstrated activity against both parasites, *Leishmania amazonensis* and *Trypanosoma cruzi*. The activity against extracellular forms ranges between $IC_{50}$ of 8.14 ± 1.2 and 28.39 ± 5.2 µM in *L. amazonensis* and from 5.06 ± 1.11 and 17.52 ± 1.71 µM in *T. cruzi*. Against the intracellular forms the most active was the compound 3 in the two parasites.

The current treatments against trypanosomatids produce several side effects, including neurological and gastrointestinal problems (Barrett

and Croft, 2012; Mathison and Bradley, 2023). For this reason, it is necessary to evaluate the cytotoxicity of the compounds to test, this varied between 34.02 ± 7.71 and 109.39 ± 24.57 μM, being the least toxic the compound 3.

Regarding the results of selectivity, the compounds that seem to give the best profile are the compounds 2 and 3 against both stage forms if the two parasites. Highlighting the selectivity indexes of compound 3 against promastigote forms of *L. amazonensis* (13.4) and against amastigote forms of *T. cruzi* (7.4).

The type of cell death produced in the parasites may condition the response of the host, since a necrotic death could produce an inflammatory process fatal for the patient. For this reason, it is important to know what kind of cell death the compounds induce in the parasites. This was evaluated with the compounds 2 and 3, for that purpose, different events involved in the apoptosis death were studied, namely, chromatin condensation, plasmatic membrane permeability and oxidative stress, among others.

The results of the different mechanisms of action demonstrate that compounds 2 and 3 induce chromatin condensation, observable in the images of Hoechst and TEM, and induce oxidative stress, which in this case is demonstrated by the presence of red fluorescence in the images with cellROX®, the amount of fluorescence is directly proportional to the amount of ROS, and thus, oxidative stress. Another important alteration occurs in the mitochondria, and this could be observed in the morphological changes with TEM images and the decrease in levels of ATP and mitochondrial membrane potential.

The plasmatic membrane is necessary to protect the cell contents. The parasites treated with the compounds 2 and 3 exhibit green fluorescence in the presence of SYTOX® Green stain, and the integrity of the cells is maintained. This disruption in the membrane permeability with maintaining the integrity of the cell is characteristic of programmed cell death.

Another striking event appear in TEM images, such as the alterations in the flagellar pocket, the high numbers of reservosomes or vacuoles, the presence of multilamellar bodies or the changes in the morphology of important organelles such as nuclei or kinetoplast, essential for the biological processes of the parasite.

All these events, the chromatin condensation, the alterations in the mitochondria, the decrease of ATP, the changes in the normal morphology of organelles, and the alterations in the plasmatic membrane, among others, are events involved in a programmed cell death. Previous studies demonstrate the induction of programmed cell death caused by acrylonitriles (Sandes et al., 2010, 2014). In addition, previous works by this group has demonstrated the existence of apoptosis like death caused by this type of compounds (Bethencourt-Estrella et al., 2021, 2022).

## 5. Conclusion

In summary, this work demonstrates that compounds 2 and 3 have activity against both forms of *L. amazonensis* and *T. cruzi*, this is consistent with previous studies in the literature, even improving on published data. In addition, the studies of mechanisms of cell death demonstrates that these compounds produce an apoptotic like cell death, which makes them good candidates for further studies. Moreover, the consistency of these data with those found in the literature makes this group of compounds, the acrylonitriles, good candidates for the design of drugs against *Leishmania* spp. and *Trypanosoma cruzi*.

## Fundings

This study was supported funded by the Consorcio Centro de Investigación Biomédica (CIBER) de Enfermedades Infecciosas (CIBERINFEC); the Instituto de Salud Carlos III, 28,006 Madrid, Spain [CB21/13/00100]; C.J.B.E [CC20230222, CABILDO.23] was funded by Cabildo Insular de Tenerife 2023–2028 and the Ministerio de Sanidad, Spain. C. J.B.E. [TESIS2020010057] was funded by a grant from the Agencia Canaria de Investigación, Innovación y Sociedad de la Información, co-funded with 85% by Fondo Social Europeo (FSE).

## Conflict of interest

The authors declare no conflict of interest.

## Appendix A. Supplementary data

Supplementary data to this article can be found online at https://doi.org/10.1016/j.ijpddr.2024.100531.

## References

Afonso, R.C., Yien, R.M.K., de Siqueira, L.B. de O., Simas, N.K., Dos Santos Matos, A.P., Ricci-Júnior, E., 2023. Promising natural products for the treatment of cutaneous leishmaniasis: a review of in vitro and in vivo studies. Exp. Parasitol. 251, 108554 https://doi.org/10.1016/j.exppara.2023.108554.

Barbosa, T.P., Junior, C.G.L., Silva, F.P.L., Lopes, H.M., Figueiredo, L.R.F., Sousa, S.C.O., Batista, G.N., da Silva, T.G., Silva, T.M.S., de Oliveira, M.R., Vasconcellos, M.L.A.A., 2009. Improved synthesis of seven aromatic Baylis-Hillman adducts (BHA): evaluation against Artemia salina Leach. and Leishmania chagasi. Eur. J. Med. Chem. 44, 1726–1730. https://doi.org/10.1016/j.ejmech.2008.03.016.

Barrett, M.P., Croft, S.L., 2012. Management of trypanosomiasis and leishmaniasis. Br. Med. Bull. 104, 175–196. https://doi.org/10.1093/bmb/lds031.

Bennis, I., Thys, S., Filali, H., De Brouwere, V., Sahibi, H., Boelaert, M., 2017. Psychosocial impact of scars due to cutaneous leishmaniasis on high school students in Errachidia province, Morocco. Infect. Dis. Poverty 6, 46. https://doi.org/10.1186/s40249-017-0267-5.

Bern, C., 2015. Chagas' disease. N. Engl. J. Med. 373, 456–466. https://doi.org/10.1056/NEJMra1410150.

Bethencourt-Estrella, C.J., Delgado-Hernández, S., López-Arencibia, A., San Nicolás-Hernández, D., Sifaoui, I., Tejedor, D., García-Tellado, F., Lorenzo-Morales, J., Piñero, J.E., 2021. Acrylonitrile derivatives against trypanosoma cruzi: in vitro activity and programmed cell death study. Pharmaceuticals 14. https://doi.org/10.3390/ph14060552.

Bethencourt-Estrella, C.J., Delgado-Hernández, S., López-Arencibia, A., San Nicolás-Hernández, D., Tejedor, D., García-Tellado, F., Lorenzo-Morales, J., Piñero, J.E., 2023. In vitro activity and mechanism of cell death induction of cyanomethyl vinyl ethers derivatives against Trypanosoma cruzi. Int. J. Parasitol. Drugs Drug Resist. 22, 72–80. https://doi.org/10.1016/j.ijpddr.2023.05.001.

Bethencourt-Estrella, C.J., Delgado-Hernández, S., López-Arencibia, A., San Nicolás-Hernández, D., Tejedor, D., García-Tellado, F., Lorenzo-Morales, J., Piñero, J.E., 2022. In vitro activity and cell death mechanism induced by acrylonitrile derivatives against Leishmania amazonensis. Bioorg. Chem. 124, 105872 https://doi.org/10.1016/j.bioorg.2022.105872.

Bruchhaus, I., Roeder, T., Rennenberg, A., Heussler, V.T., 2007. Protozoan parasites: programmed cell death as a mechanism of parasitism. Trends Parasitol. 23, 376–383. https://doi.org/10.1016/j.pt.2007.06.004.

Castelan-Ramírez, I., Salazar-Villatoro, L., Chávez-Munguía, B., Salinas-Lara, C., Sánchez-Garibay, C., Flores-Maldonado, C., Hernández-Martínez, D., Anaya-Martínez, V., Ávila-Costa, M.R., Méndez-Cruz, A.R., Omaña-Molina, M., 2020. Schwann Cell autophagy and necrosis as mechanisms of cell death by acanthamoeba. Pathogens 9. https://doi.org/10.3390/pathogens9060458.

Coles, N.T., Mahon, M.F., Webster, R.L., 2018. 1,1-Diphosphines and divinylphosphines via base catalyzed hydrophosphination. Chem. Commun. 54, 10443–10446. https://doi.org/10.1039/c8cc05890c.

Dang, Y., Li, Z., Wei, Q., Zhang, R., Xue, H., Zhang, Y., 2018. Protective effect of apigenin on acrylonitrile-induced inflammation and apoptosis in testicular cells via the NF-κB pathway in rats. Inflammation 41, 1448–1459. https://doi.org/10.1007/s10753-018-0791-x.

de Vries, H.J.C., Schallig, H.D., 2022. Cutaneous leishmaniasis: a 2022 updated narrative review into diagnosis and management developments. Am. J. Clin. Dermatol. 23, 823–840. https://doi.org/10.1007/s40257-022-00726-8.

Duan, S., Wang, Shiqi, Song, Y., Gao, N., Meng, L., Gai, Y., Zhang, Y., Wang, Song, Wang, C., Yu, B., Wu, J., Yu, X., 2020. A novel HIV-1 inhibitor that blocks viral replication and rescues APOBEC3s by interrupting vif/CBFβ interaction. J. Biol. Chem. 295, 14592–14605. https://doi.org/10.1074/jbc.RA120.013404.

Fernandes, V. de S., da Rosa, R., Zimmermann, L.A., Rogério, K.R., Kümmerle, A.E., Bernardes, L.S.C., Graebin, C.S., 2022. Antiprotozoal agents: how have they changed over a decade? Arch. Pharm. 355, e2100338 https://doi.org/10.1002/ardp.202100338.

García-Davis, S., López-Arencibia, A., Bethencourt-Estrella, C.J., San Nicolás-Hernández, D., Viveros-Valdez, E., Díaz-Marrero, A.R., Fernández, J.J., Lorenzo-Morales, J., Piñero, J.E., 2023. Laurequinone, a lead compound against Leishmania. Mar. Drugs 21. https://doi.org/10.3390/md21060333.

González-Robles, A., Salazar-Villatoro, L., González-Lázaro, M., Omaña-Molina, M., Martínez-Palomo, A., 2012. Vahlkampfia sp: structural observations of cultured trophozoites. Exp. Parasitol. 130, 86–90. https://doi.org/10.1016/j.exppara.2011.10.009.

Hagemann, C.L., Macedo, A.J., Tasca, T., 2024. Therapeutic potential of antimicrobial peptides against pathogenic protozoa. Parasitol. Res. 123, 122. https://doi.org/10.1007/s00436-024-08133-0.

Han, Y.-S., Penthala, N.R., Oliveira, M., Mesplède, T., Xu, H., Quan, Y., Crooks, P.A., Wainberg, M.A., 2017. Identification of resveratrol analogs as potent anti-dengue agents using a cell-based assay. J. Med. Virol. 89, 397–407. https://doi.org/10.1002/jmv.24660.

Junior, C.G.L., de Assis, P.A.C., Silva, F.P.L., Sousa, S.C.O., de Andrade, N.G., Barbosa, T. P., Nerís, P.L.N., Segundo, L.V.G., Anjos, I.C., Carvalho, G.A.U., Rocha, G.B., Oliveira, M.R., Vasconcellos, M.L.A.A., 2010. Efficient synthesis of 16 aromatic Morita-Baylis-Hillman adducts: biological evaluation on Leishmania amazonensis and Leishmania chagasi. Bioorg. Chem. 38, 279–284. https://doi.org/10.1016/j.bioorg.2010.08.002.

Kim, S.-M., Choi, K.-C., 2020. Acrylonitrile induced cell cycle arrest and apoptosis by promoting the formation of reactive oxygen species in human choriocarcinoma cells. J. Toxicol. Sci. 45, 713–724. https://doi.org/10.2131/jts.45.713.

López-Arencibia, A., Reyes-Batlle, M., Freijo, M.B., Sifaoui, I., Bethencourt-Estrella, C.J., Rizo-Liendo, A., Chiboub, O., McNaughton-Smith, G., Lorenzo-Morales, J., Abad-Grillo, T., Piñero, J.E., 2019a. In vitro activity of 1H-phenalen-1-one derivatives against Leishmania spp. and evidence of programmed cell death. Parasites Vectors 12, 601. https://doi.org/10.1186/s13071-019-3854-4.

López-Arencibia, A., San Nicolás-Hernández, D., Bethencourt-Estrella, C.J., Sifaoui, I., Reyes-Batlle, M., Rodríguez-Expósito, R.L., Rizo-Liendo, A., Lorenzo-Morales, J., Bazzocchi, I.L., Piñero, J.E., Jiménez, I.A., 2019b. Withanolides from withania aristata as antikinetoplastid agents through induction of programmed cell death. Pathogens 8. https://doi.org/10.3390/pathogens8040172.

López-Arencibia, A., Sifaoui, I., Reyes-Batlle, M., Bethencourt-Estrella, C.J., San Nicolás-Hernández, D., Lorenzo-Morales, J., Piñero, J.E., 2021. Discovery of new chemical tools against Leishmania amazonensis via the MMV pathogen box. Pharmaceuticals 14. https://doi.org/10.3390/ph14121219.

Luo, Y.-S., He, Q.-K., Sun, M.-X., Qiao, F.-X., Liu, Y.-C., Xu, C.-L., Xu, Z.-R., Zhao, S.-C., Wang, H.-L., Qi, Z.-Q., Liu, Y., 2022. Acrylonitrile exposure triggers ovarian inflammation and decreases oocyte quality probably via mitochondrial dysfunction induced apoptosis in mice. Chem. Biol. Interact. 360, 109934 https://doi.org/10.1016/j.cbi.2022.109934.

Manful, E.-E., Dofuor, A.K., Gwira, T.M., 2024. The role of tryptophan derivatives as anti-kinetoplastid agents. Heliyon 10, e23895. https://doi.org/10.1016/j.heliyon.2023.e23895.

Mathison, B.A., Bradley, B.T., 2023. Review of the clinical presentation, pathology, diagnosis, and treatment of leishmaniasis. Lab. Med. 54, 363–371. https://doi.org/10.1093/labmed/lmac134.

Menna-Barreto, R.F.S., 2019. Cell death pathways in pathogenic trypanosomatids: lessons of (over)kill. Cell Death Dis. 10, 93. https://doi.org/10.1038/s41419-019-1370-2.

Nakayama, H., Desrivot, J., Bories, C., Franck, X., Figadère, B., Hocquemiller, R., Fournet, A., Loiseau, P.M., 2007. In vitro and in vivo antileishmanial efficacy of a new nitrilquinoline against Leishmania donovani. Biomed. Pharmacother. 61, 186–188. https://doi.org/10.1016/j.biopha.2007.02.001.

Nicolás-Hernández, D.S., Rodríguez-Expósito, R.L., López-Arencibia, A., Bethencourt-Estrella, C.J., Sifaoui, I., Salazar-Villatoro, L., Omaña-Molina, M., Fernández, J.J., Díaz-Marrero, A.R., Piñero, J.E., Lorenzo-Morales, J., 2023. Meroterpenoids from gongolaria abies-marina against kinetoplastids: in vitro activity and programmed cell death study. Pharmaceuticals 16. https://doi.org/10.3390/ph16040476.

Organizacion Mundial de la Salud OMS, 2021. Hoja de ruta sobre enfermedades tropicales desatendidas 2021-2030. World Health Organization.

Pal, R., Teli, G., Akhtar, M.J., Matada, G.S.P., 2023. The role of natural anti-parasitic guided development of synthetic drugs for leishmaniasis. Eur. J. Med. Chem. 258, 115609 https://doi.org/10.1016/j.ejmech.2023.115609.

Penthala, N.R., Sonar, V.N., Horn, J., Leggas, M., Yadlapalli, J.S.K.B., Crooks, P.A., 2013. Synthesis and evaluation of a series of benzothiophene acrylonitrile analogs as anticancer agents. Medchemcomm 4, 1073–1078. https://doi.org/10.1039/C3MD00130J.

Pérez-Molina, J.A., Crespillo-Andújar, C., Bosch-Nicolau, P., Molina, I., 2021. Trypanocidal treatment of Chagas disease. Enferm. Infecc. Microbiol. Clín. 39, 458–470. https://doi.org/10.1016/j.eimce.2020.04.012.

Porta, E.O.J., Kalesh, K., Steel, P.G., 2023. Navigating drug repurposing for Chagas disease: advances, challenges, and opportunities. Front. Pharmacol. 14, 1233253 https://doi.org/10.3389/fphar.2023.1233253.

Saczewski, F., Stencel, A., Bieńczak, A.M., Langowska, K.A., Michaelis, M., Werel, W., Hałasa, R., Reszka, P., Bednarski, P.J., 2008. Structure-activity relationships of novel heteroaryl-acrylonitriles as cytotoxic and antibacterial agents. Eur. J. Med. Chem. 43, 1847–1857. https://doi.org/10.1016/j.ejmech.2007.11.017.

San Nicolás-Hernández, D., Bethencourt-Estrella, C.J., López-Arencibia, A., Hernández-Álvarez, E., Sifaoui, I., Bazzocchi, I.L., Lorenzo-Morales, J., Jiménez, I.A., Piñero, J. E., 2023a. Withaferin A-silyl ether analogs as potential anti-kinetoplastid agents targeting the programmed cell death. Biomed. Pharmacother. 157, 114012 https://doi.org/10.1016/j.biopha.2022.114012.

San Nicolás-Hernández, D., Hernández-Álvarez, E., Bethencourt-Estrella, C.J., López-Arencibia, A., Sifaoui, I., Bazzocchi, I.L., Lorenzo-Morales, J., Jiménez, I.A., Piñero, J.E., 2023b. Multi-target withaferin-A analogues as promising anti-kinetoplastid agents through the programmed cell death. Biomed. Pharmacother. 164, 114879 https://doi.org/10.1016/j.biopha.2023.114879.

Sandes, J.M., Borges, A.R., Junior, C.G.L., Silva, F.P.L., Carvalho, G.A.U., Rocha, G.B., Vasconcellos, M.L.A.A., Figueiredo, R.C.B.Q., 2010. 3-Hydroxy-2-methylene-3-(4-nitrophenylpropanenitrile): a new highly active compound against epimastigote and trypomastigote form of Trypanosoma cruzi. Bioorg. Chem. 38, 190–195. https://doi.org/10.1016/j.bioorg.2010.06.003.

Sandes, J.M., Fontes, A., Regis-da-Silva, C.G., de Castro, M.C.A.B., Lima-Junior, C.G., Silva, F.P.L., Vasconcellos, M.L.A.A., Figueiredo, R.C.B.Q., 2014. Trypanosoma cruzi cell death induced by the Morita-Baylis-Hillman adduct 3-Hydroxy-2-methylene-3-(4-nitrophenylpropanenitrile). PLoS One 9, e93936. https://doi.org/10.1371/journal.pone.0093936.

Sanna, P., Carta, A., Nikookar, M.E., 2000. Synthesis and antitubercular activity of 3-aryl substituted-2-[1H(2H)benzotriazol-1(2)-yl]acrylonitriles. Eur. J. Med. Chem. 35, 535–543. https://doi.org/10.1016/s0223-5234(00)00144-6.

Sharma, K., Shrivastava, A., Mehra, R.N., Deora, G.S., Alam, M.M., Zaman, M.S., Akhter, M., 2018. Synthesis of novel benzimidazole acrylonitriles for inhibition of Plasmodium falciparum growth by dual target inhibition. Arch. Pharm. 351 https://doi.org/10.1002/ardp.201700251.

Sheikh, S.Y., Hassan, F., Shukla, D., Bala, S., Faruqui, T., Akhter, Y., Khan, A.R., Nasibullah, M., 2024. A review on potential therapeutic targets for the treatment of leishmaniasis. Parasitol. Int. 100, 102863 https://doi.org/10.1016/j.parint.2024.102863.

Sivaramakarthikeyan, R., Iniyaval, S., Saravanan, V., Lim, W.-M., Mai, C.-W., Ramalingan, C., 2020. Molecular hybrids integrated with benzimidazole and pyrazole structural motifs: design, synthesis, biological evaluation, and molecular docking studies. ACS Omega 5, 10089–10098. https://doi.org/10.1021/acsomega.0c00630.

Tejedor, D., Delgado-Hernández, S., Colella, L., García-Tellado, F., 2019. Catalytic hydrocyanation of activated terminal alkynes. Chemistry 25, 15046–15049. https://doi.org/10.1002/chem.201903402.

Tretyakova, E.V., Salimova, E.V., Parfenova, L.V., Yunusbaeva, M.M., Dzhemileva, L.U., D'yakonov, V.A., Dzhemilev, U.M., 2019. Synthesis of new dihydroquinopimaric acid analogs with nitrile groups as apoptosis-inducing anticancer agents. Anti Cancer Agents Med. Chem. 19, 1172–1183. https://doi.org/10.2174/1871520619666190404100846.

Yadagiri, G., Singh, A., Arora, K., Mudavath, S.L., 2023. Immunotherapy and immunochemotherapy in combating visceral leishmaniasis. Front. Med. 10, 1096458 https://doi.org/10.3389/fmed.2023.1096458.